Table 2 Comparison of performance between CG method and Davidson's method

				CG		Davidson	
n	c	$A(1,1)$	$A(n,n)$	$F(x)$	Iter.	$F(x)$	Iter.
25	5	115.63	44.99	−5.164804107807360E+04	11	−5.164804107807630E+04	5
25	6	115.63	44.99	−4.813254329786170E+04	11	−4.813254329786540E+04	5
50	8	263.43	99.15	−4.724964225687430E+05	12	−4.724964225681190E+05	4
50	10	263.43	99.15	−4.319308443921390E+05	12	−4.319308443921450E+05	5
50	12	263.43	99.15	−4.025749894361610E+05	12	−4.025749894361660E+05	5
100	15	596.40	220.70	−3.947662073458550E+06	14	−3.947662073455790E+06	4
100	35	596.40	220.70	−3.016404837142820E+06	15	−3.016404837142080E+06	5
150	50	960.70	353.40	−1.083410906665180E+07	16	−1.083410906665080E+07	5
150	98	961.00	353.00	−1.022353967442190E+07	17	−1.022353967441990E+07	6
150	173	961.00	353.00	−1.119892218088950E+07	20	−1.119892218088840E+07	8
200	196	1347.00	494.00	−2.719539763809190E+07	19	−2.719539763808710E+07	7
200	391	1347.00	494.00	−3.953225968473330E+07	32	−3.953225968463580E+07	12
250	307	1751.00	641.00	−5.987506882057660E+07	21	−5.987506882057300E+07	8
250	571	1750.00	640.00	−9.909334646511780E+07	44	−9.909334646500030E+07	17

14) IF $flag = 0$ THEN
Return to step #3
ELSE
$[\boldsymbol{V}_{(i,1)}] = [\boldsymbol{V}^{(m)}][\boldsymbol{\alpha}^{(m)}]$
$[\boldsymbol{\alpha}^{(1)}] = 1.0$
Return to step #3
END

The variables used in the program are defined in Table 1, and a summary of the performances of the two methods is given in Table 2.

Conclusion

Davidson's method is extremely sensitive to roundoff errors and normally will not work properly if single-precision computations are used. It is extremely important that double (or higher) precision be used for this program to function properly. Arbitrary symmetric matrices were used to compare the performance of Davidson's method to the CG method. A simple program was written to construct fairly large symmetric matrices. The diagonal elements are based on the desired size of the matrix. The off-diagonal elements are constants that can be selected by the user.

Table 2 shows a summary of the performances of the two methods: the size of the matrix n, the value of the off-diagonal elements c, and the first and last diagonal elements of the matrix. The next section of Table 2 shows the values of the quadratic function $F(x)$ calculated from the approximate solution along with the number of iterations it took to converge. It is quite apparent from these results that Davidson's method outperforms the CG method as a linear solver.

Acknowledgment

This research was sponsored in part by NASA Ames Research Center under Cooperative Agreement NCC 2-937.

References

[1]Davidson, E. R., "The Iterative Calculation of a Few of the Lowest Eigenvalues and Corresponding Eigenvectors of Large Real-Symmetric Matrices," *Journal of Computational Physics*, Vol. 17, Jan. 1975, pp. 87–94.

[2]Ghosh, A., "Evaluation of Direct and Iterative Methods for Large BEM Calculations," 45th Anniversary Meeting of the Society for Industrial and Applied Mathematics, Stanford Univ., Stanford, CA, July 1997.

[3]Schwarz, H. R., Rutishauser, H., and Steifel, E., *Numerical Analysis of Symmetric Matrices*, Prentice–Hall, Englewood Cliffs, NJ, 1973, pp. 63–75.

[4]Golub, G. H., and Van Loan, C. F., *Matrix Computations*, Johns Hopkins Univ. Press, Baltimore, MD, 1993, Chaps. 6 and 8.

[5]Anton, H., and Rorres, C., *Elementary Linear Algebra—Applications Version*, Wiley, New York, 1994, pp. 320, 321.

A. Berman
Associate Editor

Delamination Fracture Toughness of Woven-Fabric Composites Under Mixed-Mode Loading

Nurudeen B. Adeyemi,* Kunigal N. Shivakumar,† and Vishnu S. Avva‡
North Carolina A&T State University, Greensboro, North Carolina 27411

Introduction

A NUMBER of composite processing techniques are being developed to reduce manufacturing costs. These techniques include compression molding, resin transfer molding, scrimp, pultrusion, etc. The new processing techniques raise the uncertainty of mechanical properties, particularly the fracture properties. Tension, compression, and shear properties of composites made from various processes were evaluated in Ref. 1. An essential property in the damage tolerance design of laminated composites is the delamination fracture toughness, which is being investigated in this Note. In laminated composite structures, delaminations initiate and propagate under a combination of normal and shear stresses due to either loading or stacking sequence. Therefore, tests of delamination resistance should account for the combined stress state.[2]

The objective of this Note is to evaluate the mode-I, -II, and mixed-mode delamination fracture toughnesses of laminated woven-fabric composites made from autoclave and compression molding processes. An autoclave-molded (ATM) composite provides the baseline data to evaluate compression-molded composites. The compression molding consists of two processes: vacuum-assisted compression molding (CMV) and no-vacuum compression molding (CM). The material used in all processes was high modulus fiber (HMF) 5322/34C carbon/epoxy prepreg. All tests were conducted using split-beam specimen and mixed-mode bending test apparatus.[3]

Material System and Specimen Fabrication

The material used in both the autoclave and compression-molding processes was HMF 5322/34C carbon/epoxy plain-weave prepreg

Presented as Paper 97-1129 at the AIAA/ASME/ASCE/AHS/ASC 38th Structures, Structural Dynamics, and Materials Conference, Kissimmee, FL, April 7–10, 1997; received July 12, 1997; revision received Nov. 15, 1998; accepted for publication Nov. 30, 1998.

*Graduate Student, Department of Mechanical Engineering, Center for Composite Materials Research.

†Research Professor, Department of Mechanical Engineering, Center for Composite Materials Research. Associate Fellow AIAA.

‡Professor, Department of Mechanical Engineering, Center for Composite Materials Research.

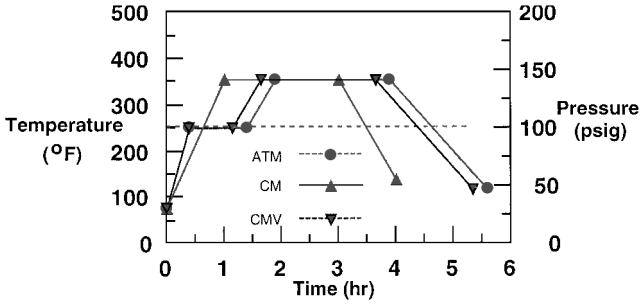

Fig. 1 Time, temperature, and pressure cycles for autoclave and compression moldings.

manufactured by Fiberite, Inc. The prepreg was made up of T300 plain-weave 3K carbon fabric and 934 epoxy. Because the yarn count per unit width and pretension were larger in the warp direction than in the fill direction, the mechanical properties are different in these two directions. To balance the stiffnesses in longitudinal and transverse directions of the laminate, the prepreg warp and fill layers were alternately stacked. The total number of layers used for 3.6-mm (0.144-in.)-thick laminate (2 h) was 20. The delamination was introduced by implanting a 50-mm (2-in.)-wide and 0.013-mm (0.5 mil)-thick Teflon® strip between the 10th and 11th plies of the prepreg stacking. Panels of size 300 × 300 mm (12 × 12 in.) were fabricated by compression molding and 200 × 350 mm (8 × 14 in.) by autoclave molding. Descriptions of autoclave and compression moldings are presented in Ref. 4. The time–temperature and time–pressure cycles used in all three processes are given in Fig. 1. Both ATM and CMV had nearly the same cure cycle. In the CM process the temperature of the prepreg was raised to 350°F at 5°F per minute, held steady at this temperature for 2 h, and then cooled to room temperature at nearly 5°F per minute. Throughout the curing process the external pressure was maintained at 100 ± 5 psi. The CMV and ATM had a vacuum cycle for about 1.25–1.5 h at 250°F and then the temperature was raised to 350°F and held for 2 h. Five panels were manufactured from each of the processes.

Fracture Test

Test Specimen

The test specimen was a split beam of width (b) 25.4 mm (1 in.) and length of about 150 mm (6 in.). The support span ($2L$) for mixed-mode and end-notched-flexure (ENF) tests was 102 mm (4 in.). The split end of the specimen was tabbed on both the top and bottom surfaces using high-quality extruded aluminum hinges. The initial delamination length (a) was about 25.4 mm (1 in.), but the actual length was measured by splitting the specimen after the test. The initial crack length ranged from 24 to 36 mm (0.94 to 1.40 in.). Thickness, width, and initial delamination lengths of all of the specimens were measured and recorded. Specimens were dried carefully in an oven at 70°C and stored in a desiccator until they were tested. At least five specimens were tested for each load condition (representing at least one specimen from each fabricated panel). Therefore, the number of specimens tested for each load condition varied from 5 to 10. Delaminated edges of the specimen were coated with water-soluble typewriter correction fluid. The initial location of the delamination front was marked by splitting the specimen with a razor blade, and then the delamination increments of 2.54 mm (0.1 in.) were marked from the apparent delamination front.

Test Apparatus

Mode-I and mode-II tests were conducted using double cantilever beam (DCB) and ENF test setups, which are very widely known (for example, Refs. 3 and 5). The mixed-mode fracture test was conducted using a modified mixed-mode bending apparatus[4] shown in Fig. 2. This apparatus combines the mode-I and the mode-II tests into one test by a lightweight and compact loading lever. Depending on the location (c) of the applied load (P_a) from the midspan of the beam, the mode mix ratio (mixity) changes from pure mode I to mode II. The relative magnitude of the loads at the beam midspan and hinged end of the lever determines the mode mixity at the delamination front.

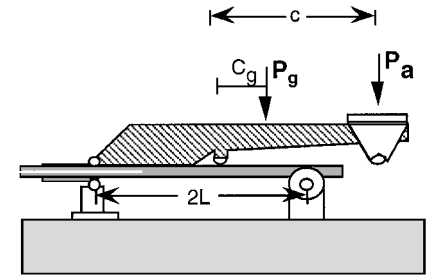

Fig. 2 Mixed-mode test apparatus and loading.

The relevant equations for strain energy release rates for DCB, ENF, and mixed-mode fracture tests are summarized next. Details of the derivation of these equations are given in Refs. 3 and 5–7.

Mode-I Strain Energy Release Rate (DCB Test)

$$G_I = \left(\frac{P_a^2}{bIE_{xx}}\right)\left(a^2 + \frac{2a}{\lambda} + \frac{1}{\lambda^2} + \frac{h^2E_{xx}}{10G_{xz}}\right) \tag{1}$$

where

$$\lambda = \frac{1}{h}\sqrt[4]{\frac{6E_{zz}}{E_{xx}}}$$

Mode-II Strain Energy Release Rate (ENF Test)

$$G_{II} = \left(\frac{3P_a^2}{64bIE_{xx}}\right)\left(a^2 + \frac{h^2E_{xx}}{5G_{xz}}\right) \tag{2}$$

Mixed-Mode Strain Energy Release Rate Test

Mode-I component:

$$G_I^m = \left(\frac{P_I^2}{bIE_{xx}}\right)\left(a^2 + \frac{2a}{\lambda} + \frac{1}{\lambda^2} + \frac{h^2E_{xx}}{10G_{xz}}\right) \tag{3}$$

Mode-II component:

$$G_{II}^m = \left(\frac{3P_{II}^2}{64bIE_{xx}}\right)\left(a^2 + \frac{h^2E_{xx}}{5G_{xz}}\right) \tag{4}$$

where

$$P_I = \left(\frac{3c - L}{4L}\right)P + \left(\frac{3c_g - L}{4L}\right)P_g$$

$$P_{II} = \left(\frac{c + L}{L}\right)P + \left(\frac{3c_g - L}{L}\right)P_g$$

where E_{xx}, E_{zz}, and G_{xz} are the longitudinal flexure, through the thickness, and transverse shear moduli, respectively; and I is the moment of inertia of half of the beam. The variables P_g and C_g represent the lever weight and the lever center of gravity from the midspan of the beam. The applied load P_a is the sum of the load applied by the test machine and the saddle weight. The P_I and P_{II} are the mode-I and mode-II components of the load.

Test Procedure

Fracture tests were conducted for mode mixity (G_I/G_{II}) ratios of 1/0 (mode I), 4/1, 2/1, 1/1, 1/4, and 0/1 (mode II). The mode-I

Table 1 Delamination fracture toughness and slope of resistance curve

G_I/G_{II}	Average G_c, J/m^2 (lb/in.)	Standard deviation	Slope of resistance curve, m, kJ/m^3 (lb/in.^{2})	Standard deviation
		Autoclave molding		
1/0 (DCB)	282.0 (1.61)	20.1	−1.92 (−0.28)	−0.24
4.33/1	336.3 (2.02)	52.1	09.31 (1.35)	0.32
2.14/1	374.8 (2.14)	65.4	17.09 (2.48)	0.58
1.13/1	385.9 (2.20)	60.1	12.42 (1.80)	0.41
1/3.48	632.7 (3.61)	74.8	Unstable	——
0/1 (ENF)	663.1 (3.79)	39.9	Unstable	——
		Compression molding		
1/0 (DCB)	375.3 (2.14)	41.0	04.21 (0.61)	0.42
4.25/1	381.9 (2.18)	62.5	11.22 (1.63)	0.46
2.12/1	439.6 (2.51)	60.7	15.79 (2.29)	0.47
1.11/1	560.4 (3.20)	104.3	05.38 (0.78)	0.27
1/3.52	746.4 (4.26)	53.3	Unstable	——
0/1 (ENF)	933.9 (5.33)	56.5	Unstable	——
		Vacuum compression molding		
1/0 (DCB)	304.3 (1.74)	87.4	09.22 (1.34)	0.46
4.29/1	315.8 (1.80)	93.4	20.53 (2.98)	0.59
2.13/1	387.0 (2.21)	52.5	27.20 (3.95)	0.78
1.13/1	558.3 (3.19)	97.9	07.47 (1.08)	0.48
1/3.49	607.7 (3.47)	29.1	Unstable	——
0/1 (ENF)	803.9 (4.59)	113.1	Unstable	——

test was conducted by pulling apart the top and bottom hinges of the split beam. The mode-II test was conducted by applying the load directly on the specimen at the midspan ($c = 0$). This test is very much like a three-point flexure test except that one end of the specimen was hinged. In the case of mixed-mode loading, the values of c corresponding to the preceding mode mixities were calculated by neglecting the lever weight (P_g) and the higher-order effects such as crack tip rotation and shear deformation. Values of c for G_I/G_{II} ratios of 4/1, 2/1, 1/1, and 1/4 were 109.5 mm (4.31 in.), 63.8 mm (2.51 in.), 44.5 mm (1.75 in.), and 28.5 mm (1.12 in.), respectively. The final ratios of G_I/G_{II} including the second-order effects and the lever weight were 4.25/1, 2.12/1, 1.11/1, and 1/3.52, respectively. The loading points were set to calculated values of c, and the load was applied by displacement control at a rate of 0.13–0.5 mm (0.005–0.02 in.) per minute. The lowest loading rate was used for ENF tests and the highest for DCB tests. The load and stroke displacement were continuously recorded using an automated data acquisition system. Loads corresponding to fracture initiation and delamination growth increments of 2.54 mm (0.1 in.) were recorded. The delamination growth was stable for tests of mode I and G_I/G_{II} of 4/1, 2/1, and 1/1 and unstable for tests of mode II and G_I/G_{II} of 1/4. After the tests the specimens were split open, and the initial delamination lengths were measured.

Separate three-point flexure tests were conducted to measure the flexure modulus of the composite specimens. Tests were conducted at low loads so that secondary deformations were neglected. The average values of E_{xx} for ATM-, CM-, and CMV-processed composites were 61.4 GPa (8.91 Msi), 54.5 GPa (7.91 Msi), and 62.2 GPa (9.02 Msi), respectively. The through-the-thickness Young's modulus E_{zz} and shear modulus were assumed to be 13.8 GPa (2 Msi) and 5.5 GPa (0.8 Msi), respectively.

Results and Discussion

Pure mode-I, mode-II, and mixed-mode fracture toughness of all specimens was computed using the maximum load of each test. The average (mean) G_c and standard deviation (STD) of all test conditions and processes are listed in Table 1. The STD of G_c for ATM-processed composites was 20.1 and 39.9 for pure mode-I and mode-II toughnesses, respectively. The STDs of G_c for CMV specimens were larger than for the other two processes. The average G_c values of ATM and CMV specimens were nearly the same for all mixed-mode loading conditions except for the mode-II condition.

Plots of G_{II}^m vs G_I^m for ATM, CM, and CMV processes are shown in Figs. 3, 4, and 5, respectively. Results on the abscissa

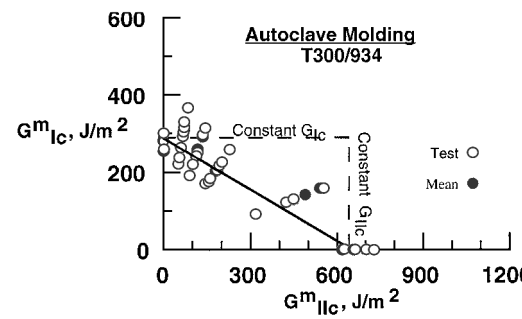

Fig. 3 Mixed-mode delamination fracture toughness envelope for ATM composites.

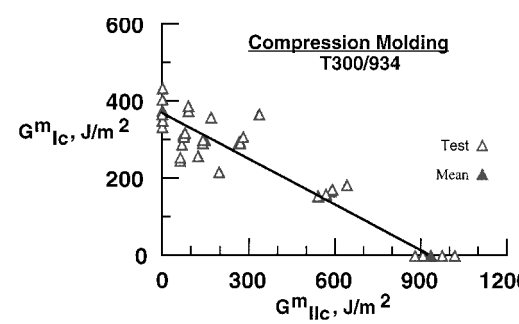

Fig. 4 Mixed-mode delamination fracture toughness envelope for CM composites.

represent the pure mode II (ENF) and on the ordinate represent the pure mode-I fracture toughnesses. Results between these two axes represent the various mixed-mode stress states. The solid symbol represents the mean value of the data. Results of the mean values fall nearly on a straight line. Figure 3 shows a comparison of constant G_{IC} and G_{IIC} and the linear Eq. (5) lines with the experimental data:

$$\left(G_I^m / G_{IC}\right) + \left(G_{II}^m / G_{IIC}\right) = 1 \tag{5}$$

The constant G_{IC} and G_{IIC} lines represent upper bound solutions. Equation (5) appears to best describe the data. Equation (5) is shown also in Figs. 4 and 5. Equation (5) best describes the mixed-mode fracture envelope of T300/934 composites.

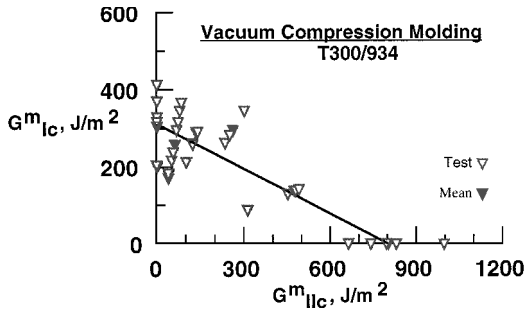

Fig. 5 Mixed-mode delamination fracture toughness envelope for CMV composites.

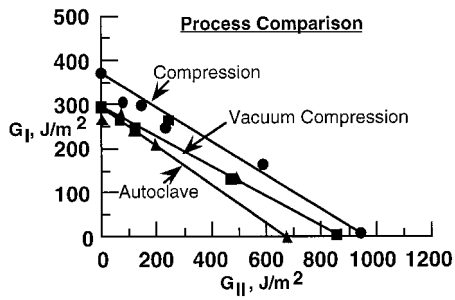

Fig. 6 Comparison of mixed-mode fracture toughness of the three processes.

A similar conclusion has been made in the literature for other brittle composites.[6]

A comparison of the processes on the mixed-mode fracture toughness is shown in Fig. 6. Only mean values are plotted. Fracture toughness of ATM composites is the lowest, followed by CVM and CM composites. The trend is the same for all values of mode mixities. To understand this trend, specimens from all three processes were compared for 1) thickness, 2) microscopic examination of edges, and 3) delamination front and fracture surfaces. Thicknesses of the CMV and CM specimens are about 5 and 10% larger than for the ATM specimens. Accordingly, layer thickness of the CMV and CM specimens will be larger than for ATM specimens. Resin thickness at the delamination front for the CM specimens was the largest, followed by that of CMV and ATM specimens; however, no significant differences were noticed in the fracture surfaces. Therefore, we can conclude that the process parameter does impact the delamination front and resin distribution through the thickness of the laminate; hence, the fracture toughnesses are different. The higher the resin content is, the larger the delamination fracture toughness will be. The difference is clearly noticeable between the ATM and CM processes.

Note that in the CM process excess resin cannot flow out of the prepreg, whereas in both ATM and CMV the vacuum expels the excess resin during the gelling process; hence, the resin content is high in CM-processed composites rather than in CMV composites. Because the CMV composites underwent nearly the same process as the ATM process, its fracture envelope falls between the ATM and CM composites but is closer to the ATM data.

Resistance Curves

As previously discussed, mode-I and mixed-mode with $G_I/G_{II} \geq 1/1$ tests showed a stable fracture, whereas the mode-II and $G_I/G_{II} \sim 1/4$ tests were unstable. Typical fracture resistance data were found to be described by a simple linear equation:

$$G_R = G_c + m\Delta a \tag{6}$$

where G_R is the fracture resistance value, G_c is the initiation fracture toughness (same as the average fracture toughness), m is the slope of the resistance curve, and Δa is the delamination growth. Depending on the values of m, the resistance is said to be constant ($m = 0$) or increasing ($m > 0$) with delamination growth.

The values of m and the data scatter in terms of STD are listed in Table 1. The slope of the resistance curve was almost zero for the mode-I condition for CM composites and a small positive value for ATM and CMV panels. The slope of the resistance curve is significant for G_I/G_{II} values between 4 and 1. The resistance curve trend is similar for all three processes, but no clear differences could be drawn because of the data scatter.

Concluding Remarks

The effect of manufacturing processes on delamination fracture toughness and resistance to growth of T300/934 plain-weave fabric carbon/epoxy laminate was evaluated. Three manufacturing processes, ATM, CM, and CMV, were used. All panels were fabricated and specimens prepared and tested under dry condition and displacement control loading. Split-edge delaminated specimens and mixed-mode bending test apparatus were used to measure delamination fracture toughness. Mode-I, -II, and mixed-mode fracture tests for G_I/G_{II} load ratios of 1/4, 1/1, 2/1, and 4/1 were conducted. Fracture tests were stable for mode I and $G_I/G_{II} \geq 1.0$ and unstable for mode II and $G_I/G_{II} \leq 1/4$. The $G^m_I/G_{IC} + G^m_{II}/G_{IIC} = 1$ best described the mixed-mode fracture envelope of T300/934 composites. Both ATM and CMV had nearly the same process conditions; hence, the fracture toughness of CMV composites was between those of ATM (closer to ATM data)- and CM-processed composites for all loading conditions. The fracture toughness of a CM composite is about 14 to 40% larger than that of ATM composites because of the larger resin thickness ahead of the delamination front. The delamination resistance of T300/934 composites can be defined by a linear equation $G_R = G_c + m\Delta a$ for $G_I/G_{II} \geq 1/1$, where G_c is the average toughness at initiation, m is the slope, and Δa is the delamination extension.

Acknowledgments

The authors acknowledge the financial support in conducting this research by the Office of Naval Research (Yapa Rajapakse, Technical Monitor) through Grant N00014-95-0649. The authors also acknowledge the Materials Directorate (James McCoy), Wright Laboratory, Wright–Patterson Air Force Base, Ohio, for providing support in c-scanning panels and specimen machining.

References

[1] Avva, V. S., "Comparative Studies on Laminated and Textile Composites," AIAA Paper 97-1322, April 1997.

[2] Salpekar, S. A., O'Brien, T. K., and Shivakumar, K. N., "Analysis of Local Delaminations Caused by Angle Ply Matrix Cracks," *Journal of Composite Materials*, Vol. 30, No. 4, 1996, pp. 419–440.

[3] Shivakumar, K. N., Crews, J. H., Jr., and Avva, V. S., "Modified Mixed-Mode Bending Test Apparatus for Measuring Delamination Fracture Toughness of Laminated Composites," *Journal of Composite Materials*, Vol. 32, No. 9, 1998, pp. 804–829.

[4] Nurudeen, A. B., Shivakumar, K. N., and Avva, V. S., "Effect of Manufacturing Process on Mixed-Mode Fracture Toughness of Woven Fabric Composites," AIAA Paper 97-1129, April 1997.

[5] Crews, J. H., Jr., and Reeder, J. R., "A Mixed-Mode Bending Apparatus for Delamination Testing," NASA TM-100662, Aug. 1988.

[6] Reeder, J. R., and Crews, J. H., Jr., "Nonlinear Analysis and Redesign of the Mixed-Mode Bending Delamination Test," NASA TM-102777, Jan. 1991.

[7] Charalambides, M., Kinloch, A. J., Wang, Y., and Williams, J. G., "On the Analysis of Mixed-Mode Failure," *International Journal of Fracture*, Vol. 54, No. 3, 1992, pp. 269–291.

A. M. Waas
Associate Editor